SUPPLEMENT 1:

DIRECT GENERATION OF ARBITRARY COMPLEX FIELDS FROM A RING LASER RESONATOR

In this supplement, we present an in-depth exposition of the optimization algorithm employed for calculating the cascaded phase holograms, ϕ_1 and ϕ_2, along with the detailed technical aspects of the experimentally constructed ring laser resonator. We first illustrate the concept of intra-cavity cascaded modulation method. Subsequently, we introduce an optimization algorithm based on a gradient-descent technique. In the algorithm's design, we discuss the determination of the positive factors α_1 and α_2 associated with the power efficiency of the zeroth-order and first-order beam generation. Finally, we outline the pump configuration of the ring resonant cavity and report on its performance metrics.

1. Concept of the intra-cavity cascaded modulation method

The beam propagation of the self-reproducing field, f_0, and the output field, f_{out}, within the ring laser resonator is illustrated in Fig. S1. The self-reproducing Gaussian field, $f_0(x_0,y_0)$, oscillating within the cavity, propagates a distance L_1 to become $f_1(x_1,y_1)$. It subsequently encounters a phase-only Spatial Light Modulator (SLM) loaded with cascaded phase holograms, ϕ_1 and ϕ_2, distanced by L_2. These holograms impart phase functions $\exp(i\phi_1(x_1,y_1))$ and $\exp(i\phi_2(x_2,y_2))$, respectively. The modulated field, $f_2(x_2,y_2)\exp(i\phi_2(x_2,y_2))$, is then Fourier transformed by a lens into $F(x_F,y_F)$ in the Fourier plane. Here, the notation (x_i,y_i) with $i = 0, 1, 2, F$ denotes the transverse coordinates at each respective plane. The transformed field $F(x_F,y_F)$ mainly comprises two diffraction orders. In the case of self-reproduction beam propagation as depicted in Fig. S1(a), the transformed field F_0 is identical to the initial field f_0. This ensures that the intra-cavity field must reproduce itself after a round-trip in the ring laser resonator. In the case of the output beam propagation depicted in Fig. S1(b), the desired output field F_1 with controllable amplitude and phase is reconstructed at the first order in the Fourier plane.

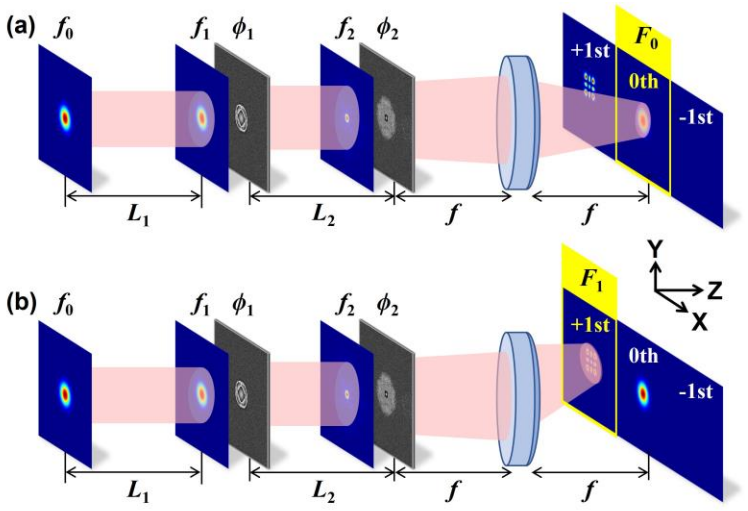

Fig. S1. Schematic diagram of the beam propagation within the laser resonator.

The notations $\mathcal{T}_{L_1}$, $\mathcal{T}_{L_2}$ and $\mathcal{T}_f$ are adopted to represent the transfer functions of free-space propagation and Fourier transform by a lens respectively. For example, under paraxial approximation, the field $f_1(x_1, y_1)$ and $F_0(x_\mathrm{F}, y_\mathrm{F})$ can be written as:

$$\begin{cases} f_1(x_1, y_1) = \iint \dfrac{f_0(x_0, y_0)}{\sqrt{i\lambda L_1}} \exp\left[\dfrac{i\pi\left((x_1 - x_0)^2 + (y_1 - y_0)^2\right)}{\lambda L_1}\right] dx_0 dy_0 \\ F_0(x_\mathrm{F}, y_\mathrm{F}) = \iint \dfrac{\left[f_2(x_2, y_2)\exp\left(i\phi_2(x_2, y_2)\right)\right]}{i\lambda f} \exp\left[\dfrac{2i\pi(x_\mathrm{F}x_2 + y_\mathrm{F}y_2)}{\lambda f}\right] dx_2 dy_2 \end{cases} . \quad \text{(S1)}$$

With the notations $\mathcal{T}_{L_1}$ and $\mathcal{T}_f$, Eq. S1 can be simplified as:

$$\begin{cases} f_1(x_1, y_1) = \mathcal{T}_{L_1}\left[f_0(x_0, y_0)\right] \\ F_0(x_\mathrm{F}, y_\mathrm{F}) = \mathcal{T}_f\left[f_2(x_2, y_2)\exp\left(i\phi_2(x_2, y_2)\right)\right] \end{cases} . \quad \text{(S2)}$$

Thus, the beam propagation as shown in Figure S1(a) can be expressed as:

$$\begin{cases} f_1(x_1, y_1) = \mathcal{T}_{L_1}\left[f_0(x_0, y_0)\right] \\ f_2(x_2, y_2) = \mathcal{T}_{L_2}\left[f_1(x_1, y_1)\exp\left(i\phi_1(x_1, y_1)\right)\right] \\ F_0(x_\mathrm{F}, y_\mathrm{F}) = \mathcal{T}_f\left[f_2(x_2, y_2)\exp\left(i\phi_2(x_2, y_2)\right)\right] \end{cases} . \quad \text{(S3)}$$

Similarly, the beam propagation in Figure S1(b) can be written as:

$$\begin{cases} f_1(x_1, y_1) = \mathcal{T}_{L_1}\left[f_0(x_0, y_0)\right] \\ f_2(x_2, y_2) = \mathcal{T}_{L_2}\left[f_1(x_1, y_1)\exp\left(i\phi_1(x_1, y_1)\right)\right] \\ F_1(x_\mathrm{F}, y_\mathrm{F}) = \mathcal{T}_f\left[f_2(x_2, y_2)\exp\left(i\phi_2(x_2, y_2)\right)\exp\left(ikx_2\gamma_S\right)\right] \end{cases} . \quad \text{(S4)}$$

Here, $kx_2\gamma_S$ denotes a phase shift introduced to spatially separate the output field $F_1(x_\mathrm{F}, y_\mathrm{F})$ from the self-reproduction field $F_0(x_\mathrm{F}, y_\mathrm{F})$ in the Fourier plane, thereby allowing distinct extraction of the desired output.

The accuracy of the transformed complex field is quantified by the normalized fidelity *Fid*, which can be calculated from the overlap integral between the target field and the transformed field. For example, the fidelity for the generation of F_1 can be expressed as:

$$Fid_{out} = \left| \frac{\iint f_\mathrm{T}(x, y) F_1^*(x, y) dxdy}{\sqrt{\iint |f_\mathrm{T}(x, y)|^2 dxdy \times \iint |F_1^*(x, y)|^2 dxdy}} \right|^2 , \quad \text{(S5)}$$

where (x, y) are the coordinates in the region of interest, f_T denotes the target output field determined as needed and the superscript $(\cdot)^*$ represents the complex conjugate. Also, for the generation of F_1, the energy efficiency is calculated by comparing the power in the transformed field to the initial field by using:

$$\eta_{\mathrm{out}} = \frac{\iint |F_1(x, y)|^2 dxdy}{\iint |f_0(x, y)|^2 dxdy} . \quad \text{(S6)}$$

Here the power of the initial field f_0 is normalized to 1 as $\iint |f_0(x, y)|^2 dxdy = 1$.

2. Optimization strategy

The algorithm is based on a gradient-descent optimization strategy that minimizes a customized cost function [1]. The cost function is chosen as follows:

$$L(\phi) = \left\| F_0(\phi) - \alpha_1 f_0 \right\|_2^2 + \left\| F_1(\phi) - \alpha_2 f_{\mathrm{T}} \right\|_2^2 \ . \tag{S7}$$

Here, ϕ symbolizes the phase holograms, having dimensions of $M \times N \times 2$, where M and N r denote the pixel counts along the x- and y- axis. $F_0(\phi)$ and $F_1(\phi)$ represent the complex fields calculated based on the phase ϕ according to Eq. S3 and Eq. S4. The powers of both the initial and target fields are normalized to unity as $\iint \left| f_0(x,y) \right|^2 dxdy = 1$ and $\iint \left| f_{\mathrm{T}}(x,y) \right|^2 dxdy = 1$, ensuring their intensities are properly scaled. The parameters α_1 and α_2 are power efficiency factors satisfying the relationship of $\alpha_1^2 + \alpha_2^2 = 1$ such that the combined theoretical power efficiency of $F_0(\phi)$ and $F_1(\phi)$ equals 100%.

The objective of the optimization is to determine the phase hologram ϕ_{opt} that minimizes $L(\phi)$, which can be concluded by:

$$\phi_{\mathrm{opt}} = \arg\min_{\phi} L(\phi). \tag{S8}$$

The optimization problem posed by Eq. S8 is inherently non-convex, and the cost function $L(\phi)$ possesses a well-defined gradient. Given this, the problem can be approached via a gradient-descent optimization algorithm. The gradient is computed for each layer of the phase holograms, specifically $\phi_j, j = 1, 2$. In the j-th plane, the cost function $L(\phi)$ can be represented in matrix form as:

$$L(\phi_j) = \left\| S_j^{\mathrm{in}}(\phi_j) \right\|_2^2 + \left\| S_j^{\mathrm{out}}(\phi_j) \right\|_2^2 \ , \tag{S9}$$

where $S_j^{in}(\phi_j) \triangleq \left(\mathbf{A}_j^{in} f_0 \exp(i\phi_j) - \alpha_1 f_0 \right)$ and $S_j^{out}(\phi_j) \triangleq \left(\mathbf{A}_j^{out} f_0 \exp(i\phi_j) - \alpha_2 f_{\mathrm{T}} \right)$ represents the difference between the transformed field and the target field. $\mathbf{A}_j^{in}$ and $\mathbf{A}_j^{out}$ is the transform matrix with size $M \times N \times j$ which stands for the linear operation from the initial field f_0 to the current field f_j, satisfying the relation of $\mathbf{A}_j^{in} f_0 = f_j^{in}$ and $\mathbf{A}_j^{out} f_0 = f_j^{out}$. The quadratic term in Eq. S9 can be expanded as:

$$L(\phi_j) = \left(S_j^{\mathrm{in}}(\phi_j) \right)^{\mathrm{H}} \left(S_j^{\mathrm{in}}(\phi_j) \right) + \left(S_j^{\mathrm{out}}(\phi_j) \right)^{\mathrm{H}} \left(S_j^{\mathrm{out}}(\phi_j) \right) \ , \tag{S10}$$

where $(\cdot)^{\mathrm{H}}$ denotes the Hermitian operator. Referring to Ref. [1], the partial derivative $\partial L(\phi_j)$ concerning the phase ϕ_j is given by:

$$\begin{aligned} \frac{\partial L(\phi_j)}{\partial \phi_j} &= S_j^{\mathrm{in}}(\phi_j)^{\mathrm{H}} \left[\frac{\partial \left(S_j^{\mathrm{in}}(\phi_j) \right)}{\partial \phi_j} \right] + S_j^{\mathrm{in}}(\phi_j) \left[\frac{\partial \left(S_j^{\mathrm{in}}(\phi_j) \right)}{\partial \phi_j} \right]^{\mathrm{H}} \\ &\quad + S_j^{\mathrm{out}}(\phi_j)^{\mathrm{H}} \left[\frac{\partial \left(S_j^{\mathrm{out}}(\phi_j) \right)}{\partial \phi_j} \right] + S_j^{\mathrm{out}}(\phi_j) \left[\frac{\partial \left(S_j^{\mathrm{out}}(\phi_j) \right)}{\partial \phi_j} \right]^{\mathrm{H}} \\ &= 2\,\mathrm{Re}\left\{ S_j^{\mathrm{in}}(\phi_j) \left[\frac{\partial \left(S_j^{\mathrm{in}}(\phi_j) \right)}{\partial \phi_j} \right]^{\mathrm{H}} \right\} + 2\,\mathrm{Re}\left\{ S_j^{\mathrm{out}}(\phi_j) \left[\frac{\partial \left(S_j^{\mathrm{out}}(\phi_j) \right)}{\partial \phi_j} \right]^{\mathrm{H}} \right\}, \end{aligned} \tag{S11}$$

where $\mathrm{Re}(\cdot)$ represents taking the real part. Thus, the gradient is calculated as:

$$\nabla_{\phi_j} L = 2\,\mathrm{Re}\left\{ \left[\frac{\partial \left(S_j^{\mathrm{in}}(\phi_j) \right)}{\partial \phi_j} \right] S_j^{\mathrm{in}}(\phi_j)^{\mathrm{H}} \right\} + 2\,\mathrm{Re}\left\{ \left[\frac{\partial \left(S_j^{\mathrm{out}}(\phi_j) \right)}{\partial \phi_j} \right] S_j^{\mathrm{out}}(\phi_j)^{\mathrm{H}} \right\}. \tag{S12}$$

By inserting $S_j^{in}(\phi_j) \triangleq \left(\mathbf{A}_j^{in} f_0 \exp(i\phi_j) - \alpha_1 f_0\right)$ and $S_j^{out}(\phi_j) \triangleq \left(\mathbf{A}_j^{out} f_0 \exp(i\phi_j) - \alpha_2 f_{\mathrm{T}}\right)$ into Eq. S11, the gradient can now be expressed as:

$$\nabla_{\phi_j} L = 2\,\mathrm{Re}\left(i\mathbf{A}_j^{\mathrm{in}} f_0 \exp(i\phi_j) S_j^{\mathrm{in}}(\phi_j)^{\mathrm{H}}\right) + 2\,\mathrm{Re}\left(i\mathbf{A}_j^{\mathrm{out}} f_0 \exp(i\phi_j) S_j^{\mathrm{out}}(\phi_j)^{\mathrm{H}}\right), \quad \text{(S13)}$$

where $S_j^{in}(\phi_j)^{\mathrm{H}}$ and $S_j^{out}(\phi_j)^{\mathrm{H}}$ is recursively calculated by backpropagation as:

$$\begin{cases} S_2^{\mathrm{in}}(\phi_2)^{\mathrm{H}} = \left\{\mathcal{T}_f\left[F_0(\phi_2) - \alpha_1 f_0\right]\right\}^{\mathrm{H}} \\ S_1^{\mathrm{in}}(\phi_1)^{\mathrm{H}} = \mathcal{T}_{L_2}\left(S_2^{\mathrm{in}}(\phi_2)^{\mathrm{H}}\right) \\ S_2^{\mathrm{out}}(\phi_2)^{\mathrm{H}} = \left\{\mathcal{T}_f\left[F_1(\phi_2) - \alpha_2 f_{\mathrm{T}}\right]\right\}^{\mathrm{H}} \\ S_1^{\mathrm{out}}(\phi_1)^{\mathrm{H}} = \mathcal{T}_{L_2}\left(S_2^{\mathrm{out}}(\phi_2)^{\mathrm{H}}\right) \end{cases}. \quad \text{(S14)}$$

Relying on Eq. S13 and Eq. S14, a quasi-Newton gradient descent algorithm is employed for the optimization purpose. This method is known for its rapid convergence and reduced computational memory demands [2]. Firstly, the cost function $L(\phi)$ is determined according to the parameters of the ring laser resonator and desired fields. Then the corresponding gradient $\nabla_\phi L$ is calculated. To facilitate this optimization, the MATLAB function *fmincon*(·) is utilized, chosen for its ease of implementation and computational efficiency.

3. Determination of the power factor

The generation of the output HG_{22} field is presented as an example for illustration of the trade-off between the power efficiency of two beam propagation processes. The transformation efficiency α_1^2 of the self-reproduction Gaussian field is designed as $\alpha_1^2 \geq 80\%$ to overcome the inherent losses in the laser cavity to achieve oscillation. The efficiency of the transformation from the Gaussian field to the desired field is defined as $\alpha_2^2 = 1 - \alpha_1^2$, thus satisfying energy conservation of 100%.

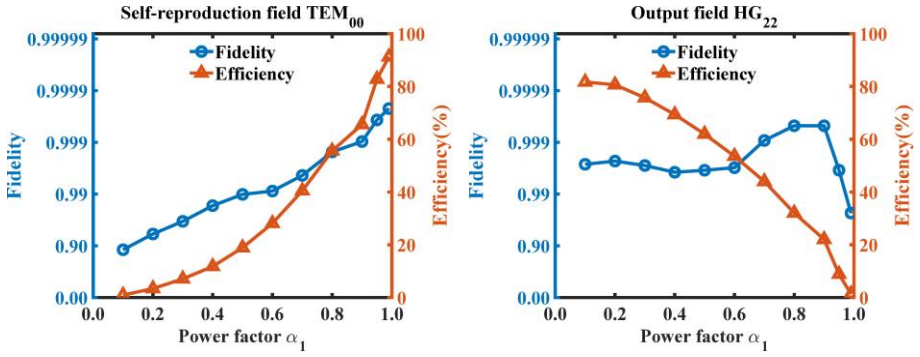

Fig. S2. Impact of the power factor α_1 on the fidelity and efficiency of the beam propagation. (a) Intra-cavity self-reproduction TEM_{00} field. (b) Extra-cavity output HG_{22} field.

The simulation outcomes are illustrated in Fig. S2, demonstrating that the efficiency of the extra-cavity HG_{22} field output decreases in tandem with the rise in the efficiency of the intra-cavity self-reproduction TEM_{00} field. To guarantee an intra-cavity mode conversion efficiency meeting the criterion $\alpha_1^2 \geq 80\%$, α_1 should be set as high as 0.90. Note that the total efficiency would be less than 100% after optimization. The main reason is that part of the energy is redistributed to other diffraction orders other than the desired +1 diffraction order. Nonetheless, the optimization algorithm is instrumental in securing a sufficiently high intra-cavity mode conversion efficiency to surmount inherent cavity losses and sustain oscillation.

4. Pump scheme and performance metrics of the ring laser system

In our study, it is assumed that the gain distribution within the Nd:YAG active medium is uniform. The Nd:YAG crystal utilized in our experiments originates from a commercial module, the layout of which is depicted in Fig. S3(a). Here, the Nd:YAG rod is enveloped by five arrays of laser diode bars, each operating at a central wavelength of 808 nm, ensuring homogeneous pumping as illustrated in Fig. S3(b). This pumping configuration guarantees a high degree of gain uniformity. Considering the thermal effects inherent to Nd:YAG, our approach employs quasi-continuous pumping instead of continuous pumping, complemented by water cooling, to mitigate heat accumulation. Operated at a pump voltage of 18V and current of 22A with a duty cycle of 10%, the average pump power approximates 39.6W, under which conditions thermal effects in the Nd:YAG can be neglected.

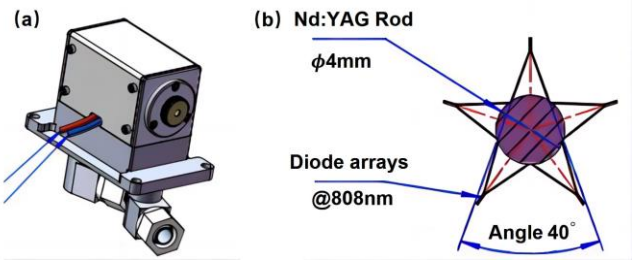

Fig. S3 (a) Schematic illustration of the Nd:YAG module; (b) Diagram of the pumping arrangement.

Output power serves as a crucial indicator of the resonator's operational efficiency. In the ring cavity designed for this work, taking the HG_{11} mode as an illustrative case, the relationship between the output power and pump power is depicted in Figure S4. Under conditions of a pump voltage of 18 V, a pump current of 22 A, and a duty cycle of 10%, the average output power reaches 118mW. Moreover, the curve reveals a pump threshold of approximately 32.6 W and a slope efficiency of about 1.71%. The principal reason for the relatively low slope efficiency lies in the necessity to ensure effective oscillation of the fundamental mode within the cavity; thus, the power conversion factor α_2^2, representing the transformation from the fundamental mode to the output mode, is set below 20%, leading to a reduced output power.

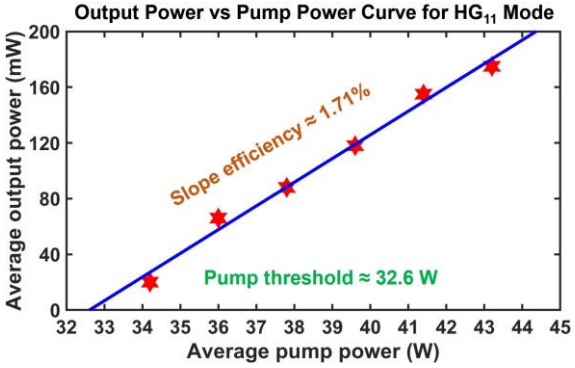

Fig. S4 Performance curve of the ring laser in generating the HG_{11} mode

References

1. C. Hu, Y. Xiao, Y. He, Y. Hu, G. Xu, and X. Tang, "Generation of arbitrary complex fields with high efficiency and high fidelity by cascaded phase-only modulation method," Opt. Express **31**(4), 6675 (2023).
2. F. E. Curtis and X. Que, "A quasi-Newton algorithm for nonconvex, nonsmooth optimization with global convergence guarantees," Math. Prog. Comp. **7**(4), 399–428 (2015).